------Raf. Jour. Sci., Vol.18, No. 1, pp.59-67, 2006------

Design Enhancement of the 460 GHz, Second Harmonic Gyrotron Oscillator Through Its Dispersion Diagram

Aras S. Mahmood **Raz N. Arif**
Department of Physics
College of Science
Sulaimani University

(Received 16/3/2006 , Accepted 12/3/2007)

ABSTRACT

All high power radio frequency (RF) sources have their own dispersion diagram, giving the relation between the output frequency (w) of the device and the axial wave number component (k_z) of the operating waveguide wave mode. This diagram gives the most important characteristics about the source and in this work it was used as a tool for the device design enhancement. From this diagram one can change the input design parameters in order to get the best dispersion diagram fitting with standard one. In this work, the dispersion diagram for the 460 GHz second harmonic gyrotron oscillator studied previously by Hornstein (2001) was plotted and the main characteristics of these kinds of gyrotrons were observed from the diagram which replies the precision of the design.

تعزيز التصميم لمرنان جايروترون التوافقية الثانية 460 GHz من خلال الرسم البياني للتقزح

الملخص

يعتبر الجايروترون مصدرا مهما من مصادر القدرة العالية للموجات الراديوية المتشاكة. تتفاعل الموجات الراديوية (RF) داخل تجويف المرنان مع حزمة الالكترونات حيث تتحول الطاقة الحركية المستعرضة الى حزمة من الموجات الراديوية. ان كل مصدر من هذه المصادر يملك رسما بيانيا للتقزح الخاص به والذي يعطي العلاقة بين تردد الموجة الخارجة (W) للمصدر والمركبة الافقية للعدد الموجي (K_z) لنمط دليل الموجة الموجودة داخل المرنان.

الرسم البياني للتقزح يبين اهم خصائص هذه المصادر, لذا يمكن استخدام هذه الفكرة كوسيلة لتعزيز تصميم الجايروترون. رسم فى هذا البحث رسما بيانيا لمرنان جايروترون التوافقية الثانية عند 460 GHz والمصمم سابقا وتبين من الرسم البياني توافر اهم الخصائص والشروط اللازمة لهذا النوع من الجايروترون وبالتالي اظهر دقة التصميم.

INTRODUCTION

The gyrotron is a microwave device based on the cyclotron maser interaction between an electromagnetic wave and an electron beam in which the individual electrons move along helical trajectories in the presence of an applied axial magnetic field ($B_\circ$). It has emerged as a new and by far the most powerful source of coherent millimeter (30 – 300) GHz and sub millimeter ($\rangle 300$ GHz) radiation (Chu et al., 1980).

The condition of coherent radiation is that the contribution from the electrons reinforces the original emitted radiation in the oscillator or the incident electromagnetic wave in the gyrotron amplifier (Granatstein and Alexeff, 1987). This radiation is satisfied if a bunching mechanism exists to create electron density variations of a size comparable to the wavelength of the imposed electromagnetic wave. To achieve such a mechanism (bunching mechanism), a resonance condition must be satisfied between the periodic motion of the electrons and the electromagnetic wave in the interaction region (Thumm, 2002).

The interaction between a beam of gyrating electrons, in the presence of a background DC magnetic field and an electromagnetic wave can lead to extraction of the transverse kinetic energy of the electrons. This interaction known as the Cyclotron Resonance Maser (CRM) instability (Felch et al., 1999). The CRM mechanism produces phase bunching by the change in the relativistic mass of the electrons as they gain or lose energy from the transverse electric field in the waveguide (Sirigiri, 1999). As the devices are increased toward a commercial reactor size and performance of experimental, the requirements for frequency and unit output power of gyrotrons also tighten. It is therefore important to know the operational limits of such gyrotrons (Airila, 2003). A number of novel devices like gyro-TWT, gyro-klystron, gyro-twystron are being considered. Irrespective of the type of the RF device, the starting point for RF power production is the selection of the design parameters of the gun and the cavity resonator. The accuracy and the precision of the design can be controlled through the study of the dispersion diagram of the device and from the calibration of this diagram with the standard one. Steven and Nusinovich (1997) gave the dispersion diagram for the Cherenkov devices like Traveling Wave Tube (TWT) and Backward Wave Oscillators (BWOs) with a sufficient explanation and importance of that diagram. A special case of interaction of gyrating electrons with the resonator field at two cyclotron harmonics simultaneously, in contrast to conventional cyclotron resonance at only one harmonic was mentioned briefly by (Nusinovich et al., 1995). Nusinovich and Zhao, 1988 plotted the dispersion diagram of such a device, illustrating the double resonance of one resonator mode followed by two traveling waves with an electron beam at two cyclotron harmonics.

THEORY

Many configurations beside gyrotron oscillator like gyro-TWT, gyro-klystron, gyro-twystron, gyro-peniotron and Cyclotron Autoresonance Maser (CARM) can be used to produce coherent radiation based on the Electron Cyclotron Maser instability. The departure point for design based on a particular concept is the wave-particle interaction (Sirigiri, 1999). The microwave frequency w of the device and the cyclotron frequency

w_c of an electron intimately related by the Eqn. (1) known as the resonance condition equation (Felch et al., 1999).

$$w - k_z v_z = s\, w_c \tag{1}$$

Where s =1, 2…etc. and $k_z v_z$ is Doppler term. w and k_z are the wave angular frequency and the characteristic axial wave number, respectively, v_z is the axial component of the electron drift velocity, w_c is the cyclotron frequency, which is associated with macroscopic motion of the electrons, and s is the harmonic number. Dispersion diagrams, also called $w - k_z$ plots, or Brillouin diagrams (Granatstein and Alexeff, 1987), show the region of the interaction (maximum gain of the instability) between an electromagnetic mode and a fast electron cyclotron mode (fundamental or harmonic).

The waveguide mode dispersion curve (hyperbola) given by equation (2):

$$w^2 = k_z^2 c^2 + k_\perp^2 c^2 \tag{2}$$

With the beam-wave resonance line (straight) given by equation (1). In the case of a device with cylindrical resonator the perpendicular wave number ($k_\perp$) given by:

$$k_\perp = \frac{X_{mn}}{R_\circ} \tag{3}$$

Where (X_{mn}) is the nth root of the corresponding Bessel function (TM_{mn} modes) or derivative of Bessel function (TE_{mn} modes) and $R_\circ$ is the waveguide or the cavity radius. Phase synchronism of the two waves is given in the intersection region (Thumm, 2002).

The different electron cyclotron maser (ECM) devices are classified according to dispersion diagrams. Sirigiri (1999) used the diagram as a tool to distinguish between the Gyro-TWT and CARM sources in the view of their interaction region. From Fig.(1), it is clear that for the CARM the region is very close to the light line while the Gyro-TWT region prevails very close to the wave guide cut-off.

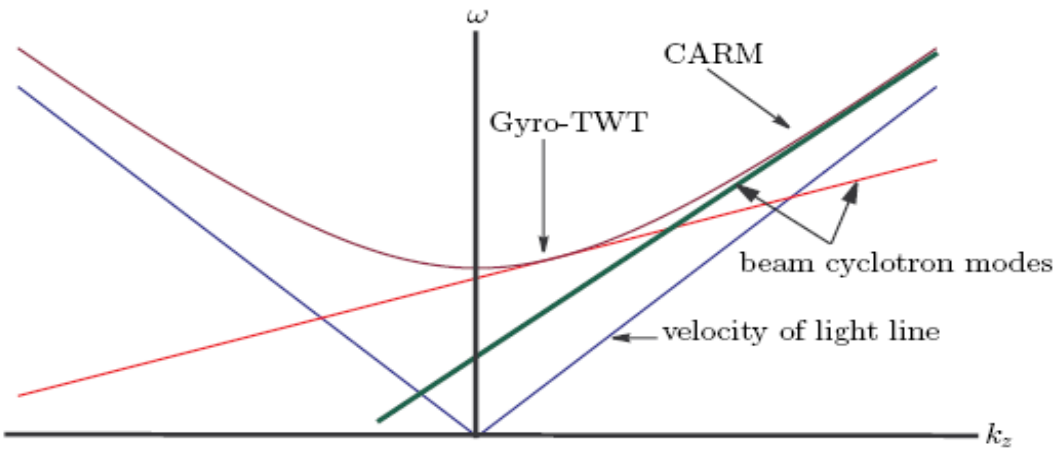

Fig. 1: Dispersion diagram showing the interaction region between a fast waveguide mode and a beam cyclotron mode in a gyro-TWT and a CARM. The gyro-TWT interaction takes place near the waveguide cut-off while the CARM interaction takes place far away from the waveguide cut-off.

The beam mode dispersion relation and the waveguide mode dispersion relations have been plotted for different kinds of cyclotron resonance maser (CRM) devices by Sirigiri (2003) and shown in Figs. (1-3). The interaction in all these devices except the Slow Wave Cyclotron Amplifier (SWCA) is very similar. In the SWCA (Fig.2) the electron bunching occurs due to the Weibel mechanism and is axial in contrast to the transverse bunching dominant in a CRM.

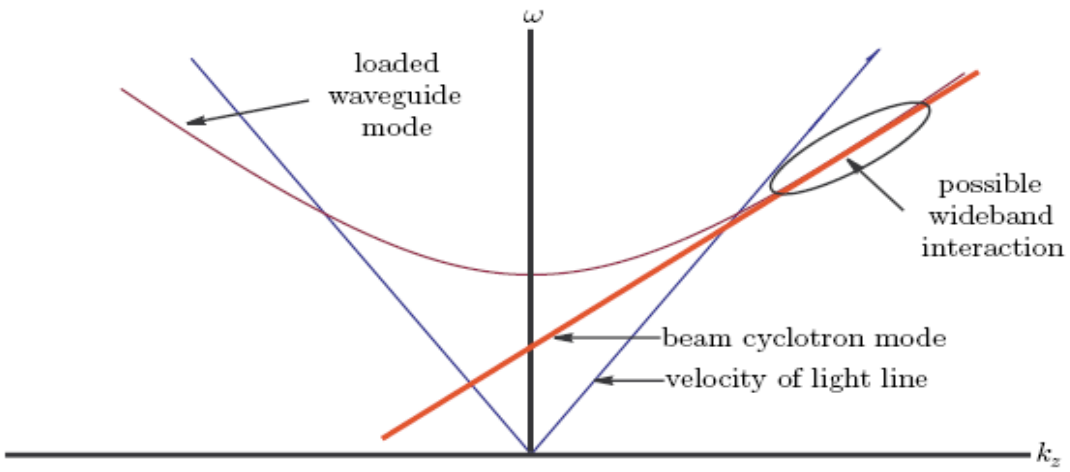

Fig. 2: Dispersion diagram showing the interaction region between a slow waveguide mode and a beam cyclotron mode in a slow-wave cyclotron amplifier (SWCA).

The dispersion diagram shown in the Fig. (3) applies to both CRM amplifiers (convective instability), oscillators (absolute instability and Backward Propagating Wave Oscillator). The intersection of the beam mode dispersion relation with the waveguide mode at a negative value of the axial propagation constant can excite Backward Propagating Wave Oscillations (BPWO) (Sirigiri, 2003).

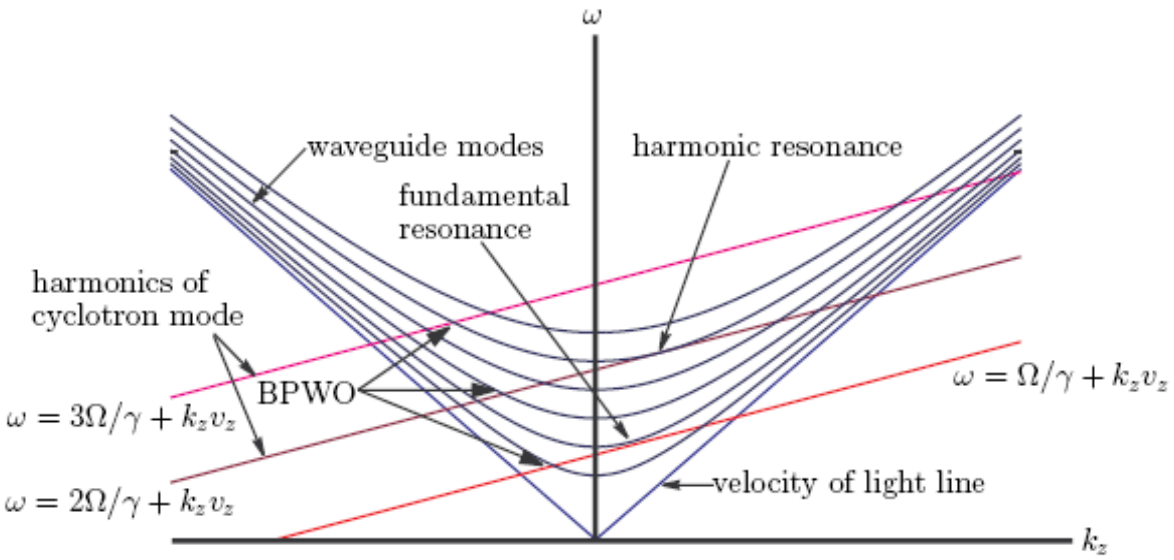

Fig. 3: Dispersion diagram showing the region of interaction between the fast waveguide modes and the beam cyclotron modes on the beam. The intersection of the beam cyclotron modes with the waveguide modes at negative values of *kz* causes the excitation of Backwad Propagating Wave Oscillations (BPWO).

DISPERSION DIAGRAM OF THE 460 GHz

The dispersion relation for the operating waveguide mode (TE_{061}) for the 460 GHz second harmonic gyrotron oscillator (designed by Hornstein, 2001) was created by plotting the dispersion relation of the waveguide mode $\left(w^2 = k^2 c^2\right)$ together with the beam-wave resonance line $\left(w - k_z v_z = 2w_c\right)$ as follows:

The cyclotron frequency (w_c) of the electron is given by Hakkarainen et al., 1990 as:

$$w_c = \frac{c\overline{B}_\circ}{\gamma_{rel} R_\circ} \qquad (4)$$

Where γ_{rel} is the relativistic mass factor $\left(\gamma_{rel} = 1/\sqrt{1 - v^2/c^2}\right)$ and tabulated in Table (1) for 18 representative electrons by using the computer program (GYROTRON 1) (Mahmood, 2005). From Table (1) the average value of γ_{rel} is 1.0215.

$\overline{B}_\circ$ is the normalized (unit less) axial magnetic field given by Chu et al., 1980 as:

$$\overline{B}_\circ = B_\circ \frac{eR_\circ}{mc} \qquad (5)$$

Where e, m are the charge and the rest mass of the electrons while c is the velocity of light.

Using the input design parameters values of Table (2) (Hornstein, 2001) one can find $\overline{B}_{\circ}$=10.0267 and from Eqn. (4):

w_c =1443.4799 GHz.

From Eqn. (1), for $w=0$ and using the laboratories frame of references (i.e. k_{z1}, v_{z1} instead of k_z, v_z):

$$k_{z1} = -\frac{2w_c}{v_{z1}} \tag{6}$$

Table 1: The axial velocity and the relativistic mass factor of the 18 representative electrons.

No. of the electrons	**Axial electron velocity (v_{z1}) c**	**Relativistic mass factor (γ_{rel})**
1	0.0980	1.0216
2	0.0980	1.0224
3	0.0980	1.0233
4	0.0980	1.0224
5	0.0981	1.0256
6	0.0982	1.0271
7	0.0982	1.0280
8	0.0981	1.0261
9	0.0981	1.0195
10	0.0984	1.0129
11	0.0981	1.0277
12	0.0979	1.0230
13	0.0980	1.0172
14	0.0982	1.0152
15	0.0981	1.0159
16	0.0980	1.0174
17	0.0980	1.0191
18	0.0980	1.0206

Where v_{z1} is the average axial velocity of the 18 representative electrons (Table 1) and is equal to 0.098078 c $\left(0.098078\times 3\times 10^{10}\right)$.

Table 2: Gyrotron cavity design parameters.

Mode	TE_{061}
Frequency (GHz)	460
Magnetic Field (T)	8.39
Diffractive Q	37,770
Total Q	12,950
Cavity Radius (mm)	2.04
Cavity Length (mm)	25

From Eqn. (6):

$$k_{z1} = \frac{2w_c}{v_{z1}} = \frac{2 \times 1443.4799 \times 10^9}{0.098078 \times 3 \times 10^{10}} = 981.178 \ m^{-1}$$

The cutoff frequency $w_{c\circ}$ (The frequency above which there is no wave propagation i.e. k_z=0) of the operating mode (TE_{061}) was calculated from Eqn. (2) as:

$$w^2 = k_z^2 c^2 + k_\perp^2 c^2$$

For $k_z = 0$

$$w^2 = k_\perp^2 c^2 = w_{c\circ}^2$$

Substituting $k_\perp$ from Eqn. (3) in the above Eqn.

$$w_{c\circ}^2 = \frac{X_{mn}^2}{R_\circ^2} c^2 \qquad (7)$$

For the studied operating mode (TE_{061} mode), $X_{mn} = X_{06}$ and is equal to 19.6172 (Mahmood, 2005) and from Eqn. (7), the cutoff frequency $w_{c\circ} = 2885$ GHz. Using the above values of k_{z1} (for w=0) and $w_{c\circ}$ with a proper FORTRAN program (Mahmood, 2005) the dispersion diagram (w versus k_{z1}) for the 460 GHz gyrotron was

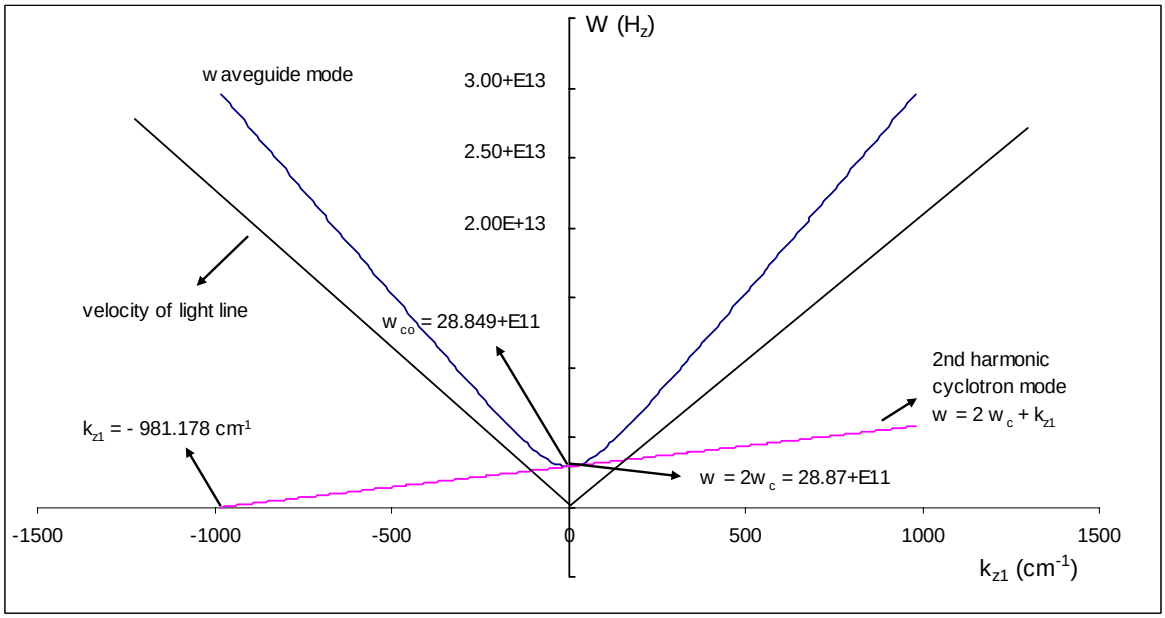

Fig. 4: The dispersion diagram for the 460 GHz second harmonic gyrotron oscillator.

CONCLUSION

From the dispersion diagram given in (Fig. 4) the following points are the most important characteristics of the gyrotron oscillators were observed and satisfied. From the study of the following points one can ensure that the new design carries the characteristics of the gyrotron oscillators. This idea was used as a tool for the design accuracy enhancement and to emphasize on the precision of the input design parameters values of the new gyrotron. The points are:

1- The fast wave device:

From the Fig. (4), the intersection of the waveguide mode and the 2nd harmonic cyclotron mode is above the line of the velocity of light which indicates that the device is the fast wave device .i.e. the phase velocity of the wave produced by this device is greater than the speed of light which must be the case for all gyrotron oscillators.

2- The near cutoff frequency operation:

Gyrotron oscillators, characterized by operating near the cutoff frequency (w_{co}) that is the operating frequency $(w = 2\pi f)$, is too close to the cutoff frequency (w_{co}) of the waveguide mode. For the studied gyrotron the operating frequency equals 460 GHz so:

$$w = 2\pi f = 2 \times 3.14 \times 460 = 2888 \text{ GHz}$$

and from the calculations in the previous section $w_{c_\circ} = 2885$ GHz. These two values (w) and (w_{co}) are close to each other satisfying the second gyrotron oscillators characteristics.

3- The interaction region:

It is clear that the point of intersection of the beam-wave line and the waveguide mode curve is in the positive k_{z1} values. This is the case for fast wave devices in contrast to the slow wave devices for which k_{z1} is negative.

REFERENCES

Airila, M.I., 2003. Degradation of Operation Mode Purity in a Gyrotron with an Off-axis Electron Beam Physics of Plasmas, Vol. 10, No. 1, pp.296-299.

Chu, K.R., Read, M.E. and Ganguly, A.K., 1980. Methods of Efficiency Enhancement and Scaling for the Gyrotron Oscillator., IEEE Transaction on Microwave Theory and Techniques, Vol. MTT-28, No. 4, pp.318-325.

Felch, K.L., Danly, B.G., Jory, H.R., Kreischer, K.E., Lawson, W., Levush, B. and Temkin, R.J., 1999. Characteristics and Applications of Fast-Wave Gyrodevices, IEEE., Vol. 87, No. 5, pp.752-781.

Granatstein, V.L. and Alexeff, I., 1987. High- Power Microwave Sources, Artech House Boston. London, 564 p.

Hakkarainen, S.S., Kreischer, K.E. and Temkin, R.J., 1990. Submillimeter Wave Harmonic Gyrotron Experiment, IEEE Trans. Plasma Sci., Vol. 18, pp.334-342.

Hornstein, M.K., 2001. Design of a 460 GHz Second Harmonic Gyrotron Oscillator for Use in Dynamic Nuclear Polarization, M.Sc. Thesis, MIT. USA. 96 p.

Mahmood, A.S., 2005. Design Study of the 455 GHz, 1.027 kW Second Harmonic Gyrotron Oscillator., Ph.D. Thesis, University of Sulaimani, Sulaimani / Iraq. 170 p.

Nusinovich, G.S. and Zhao, J., 1988. Double Resonance in Cyclotron Resonance Masers, Physical Review, Vol. 58, No. 1, pp.1002- 1010.

Nusinovich, G.S., Latham, P.E., Latham and Dnmbrajs, O., 1993. Some Concepts of Relativistic Gyroamplifiers for Practical Acceleration., Laboratory for Plasma Research, University of Maryland, College Park, MD 20742, pp.2673-2674.

Sirigiri, J.R., 1999. Theory and Design Study of a Novel Quasi-Optical Gyrotron Traveling Wave Amplifier., M.Sc. Thesis, MIT, USA. 125 p.

Sirigiri, J.R., 2003. A Novel Wideband Gyrotron Traveling Wave Amplifer., Ph.D. Thesis, MIT, USA. 214 p.

Steven, H.G. and Nusinovich, G.S., 1997. Review of High- Power Microwave Source Research., Rev. Sci. Instr, Source Research., Rev. Sci. Instr, Vol. 68, No. 11, pp.3945 – 3973.

Thumm, M.K., 2002. State of the Art of High Power Gyro Devices and Free Electron Masers., Technical Report, Forschungszentrum Karlsruhe in der Helmholtz-Gemeinschaft, Wissenschaftliche Berichte, FZKA 6815, 83 p.